ISSN 1990-4789, Journal of Applied and Industrial Mathematics, 2022, Vol. 16, No. 3, pp. 440–448. © Pleiades Publishing, Ltd., 2022.
Russian Text © The Author(s), 2022, published in Sibirskii Zhurnal Industrial'noi Matematiki, 2022, Vol. 25, No. 3, pp. 55–66.

Mathematical Simulation of Nuclear Carbon Burning in White Dwarfs Using a 7-Isotope Reaction Network

I. M. Kulikov[1*], I. G. Chernykh[1], I. S. Ulyanichev[1***], and A. V. Tutukov[2****]**

[1] *Institute of Computational Mathematics and Mathematical Geophysics, Siberian Branch, Russian Academy of Sciences, Novosibirsk, 630090 Russia*

[2] *Institute of Astronomy, Moscow, 119017 Russia*

*e-mail: *kulikov@ssd.sscc.ru, ** chernykh@parbz.sscc.ru, *** wmzonacomvn@mail.ru, **** atutukov@inasan.ru*

Received January 11, 2022; revised February 13, 2022; accepted June 22, 2022

Abstract—The mechanism of explosion of type Ia supernovae is based on nuclear burning of the white dwarf material. When modeling scenarios for the evolution of white dwarfs followed by a supernova explosion, it is important to fully take into account the nonequilibrium chemical kinetics of major isotopes in the form of subgrid processes. It is necessary to consider a detailed network of nuclear reactions, but in this case not all reactions make major contributions both to the final mass fraction of isotopes and to the energy of burning. However, even the conventional 7-, 13-, 19-, 21-, or 34-isotope networks of reactions present a rather expensive procedure of subgrid processes to consider. We propose a "convolution" of an alpha network of nuclear reactions whose analytical form can be used in a hydrodynamic model of the evolution of white dwarfs and a type Ia supernova explosion. A large number of computational experiments with a distributed client-server computational system is used to construct such a model.

Keywords: *computational astrophysics, computational chemistry, white dwarf, alpha network of nuclear reactions, isotope*

DOI: 10.1134/S1990478922030085

INTRODUCTION

Type Ia supernovae are the main source of "life" elements in the Universe. Mathematical modeling of such phenomena requires, in addition to a detailed calculation of hydrodynamic flows, taking into account the nuclear combustion reactions of the material of white dwarfs in the form of subgrid processes. However, in a computational model, the use of some complex network of chemical reactions often leads to an unbearable computational load. The paper [1] experimentally and theoretically substantiated the importance of taking into account the following isotopes: ^{12}C, ^{16}O, ^{20}Ne, ^{24}Mg, ^{28}Si, ^{56}Ni, and alpha particles ^{4}He. These are the key elements in nucleosynthesis both in terms of observations and in terms of the energetics of nuclear reactions.

Of especial importance is the chemical composition of the remnant in type Iax supernovae [2, 3], which are quite often formed in collisions of white dwarfs [4]. Of particular note is the problem of nickel production in dwarf galaxies [5] and in supernova remnants obtained in double detonation [6, 7] and of iron in Chandrasekhar supernovae [8], and also chemical composition of the combustion front of the material [9], its stability [10], and its ignition [11]. The model of the chemical evolution of the main isotopes constructed in this paper together with the model of turbulent combustion of white dwarf material [12, 13] permits one to obtain an efficient model for describing the evolution of type Ia supernovae from the explosion scenario to the propagation of the remnant.

In the first section, we describe the mathematical model of a network of nuclear reactions. The second section deals with distributed computing systems. The third section presents the main computational experiments. In the fourth section, we construct "convolution" models of nuclear reactions and also consider debatable issues. In the summary, we give the main conclusions concerning this paper.

1. 7-ISOTOPE MATHEMATICAL MODEL OF CARBON BURNING

We will consider seven key isotopes ^{4}He, ^{12}C, ^{16}O, ^{20}Ne, ^{24}Mg, ^{28}Si, and ^{56}Ni and the following set of alpha-chain nuclear reactions:

1. Nuclear burning of helium: $3 \times {}^4\mathrm{He} \to {}^{12}\mathrm{C} + \gamma$.
2. Synthesis of oxygen from carbon: ${}^{12}\mathrm{C} + {}^4\mathrm{He} \to {}^{16}\mathrm{O} + \gamma$.
3. Synthesis of neon from oxygen: ${}^{16}\mathrm{O} + {}^4\mathrm{He} \to {}^{20}\mathrm{Ne} + \gamma$.
4. Synthesis of magnesium from neon: ${}^{20}\mathrm{Ne} + {}^4\mathrm{He} \to {}^{24}\mathrm{Mg} + \gamma$.
5. Synthesis of silicon from magnesium: ${}^{24}\mathrm{Mg} + {}^4\mathrm{He} \to {}^{28}\mathrm{Si} + \gamma$.
6. Nuclear burning of carbon: ${}^{12}\mathrm{C} + {}^{12}\mathrm{C} \to {}^{24}\mathrm{Mg}$.
7. Nuclear combustion of carbon and oxygen: ${}^{12}\mathrm{C} + {}^{16}\mathrm{O} \to {}^{28}\mathrm{Si}$.
8. Nuclear combustion and synthesis of oxygen to nickel: ${}^{16}\mathrm{O} + {}^{16}\mathrm{O} + 6 \times {}^4\mathrm{He} \to {}^{56}\mathrm{Ni} + 6\gamma$.
9. Nuclear combustion and synthesis of silicon to nickel: ${}^{28}\mathrm{Si} + 7 \times {}^4\mathrm{He} \to {}^{56}\mathrm{Ni} + 7\gamma$.
10. Silicon photodisintegration: ${}^{28}\mathrm{Si} + \gamma \to {}^{24}\mathrm{Mg} + {}^4\mathrm{He}$.
11. Magnesium photodisintegration: ${}^{24}\mathrm{Mg} + \gamma \to {}^{20}\mathrm{Ne} + {}^4\mathrm{He}$.
12. Neon photodisintegration: ${}^{20}\mathrm{Ne} + \gamma \to {}^{16}\mathrm{O} + {}^4\mathrm{He}$.
13. Oxygen photodisintegration: ${}^{16}\mathrm{O} + \gamma \to {}^{12}\mathrm{C} + {}^4\mathrm{He}$.
14. Carbon photodisintegration: ${}^{12}\mathrm{C} + \gamma \to 3 \times {}^4\mathrm{He}$.
15. Nickel photodisintegration: ${}^{56}\mathrm{Ni} + 7\gamma \to {}^{28}\mathrm{Si} + 7 \times {}^4\mathrm{He}$.

The table of reaction rates k_i and released energy Q_i can be found in [14]. We will consider the following system of ordinary differential equations written for the evolution of the mass fraction of each element $M_{^4\mathrm{He}}$, $M_{^{12}\mathrm{C}}$, $M_{^{16}\mathrm{O}}$, $M_{^{20}\mathrm{Ne}}$, $M_{^{24}\mathrm{Mg}}$, $M_{^{28}\mathrm{Si}}$, and $M_{^{56}\mathrm{Ni}}$:

$$\begin{aligned}\frac{dM_{^4\mathrm{He}}}{dt} = {}& -3k_1M_{^4\mathrm{He}}^3 - k_2M_{^{12}\mathrm{C}}M_{^4\mathrm{He}} - k_3M_{^{16}\mathrm{O}}M_{^4\mathrm{He}} - k_4M_{^{20}\mathrm{Ne}}M_{^4\mathrm{He}} \\ & - k_5M_{^{24}\mathrm{Mg}}M_{^4\mathrm{He}} - 6k_8M_{^{16}\mathrm{O}}^2M_{^4\mathrm{He}}^6 - 7k_9M_{^{28}\mathrm{Si}}M_{^4\mathrm{He}}^7 + k_{10}M_{^{28}\mathrm{Si}} \\ & + k_{11}M_{^{24}\mathrm{Mg}} + k_{12}M_{^{20}\mathrm{Ne}} + k_{13}M_{^{16}\mathrm{O}} + 3k_{14}M_{^{12}\mathrm{C}} + 7k_{15}M_{^{56}\mathrm{Ni}},\end{aligned} \tag{1}$$

$$\frac{dM_{^{12}\mathrm{C}}}{dt} = k_1M_{^4\mathrm{He}}^3 - k_2M_{^{12}\mathrm{C}}M_{^4\mathrm{He}} - 2k_6M_{^{12}\mathrm{C}}^2 - k_7M_{^{12}\mathrm{C}}M_{^{16}\mathrm{O}} + k_{13}M_{^{16}\mathrm{O}} - k_{14}M_{^{12}\mathrm{C}}, \tag{2}$$

$$\frac{dM_{^{16}\mathrm{O}}}{dt} = k_2M_{^{12}\mathrm{C}}M_{^4\mathrm{He}} - k_3M_{^{16}\mathrm{O}}M_{^4\mathrm{He}} - k_7M_{^{12}\mathrm{C}}M_{^{16}\mathrm{O}} - 2k_8M_{^{16}\mathrm{O}}^2M_{^4\mathrm{He}}^6 + k_{12}M_{^{20}\mathrm{Ne}} - k_{13}M_{^{16}\mathrm{O}}, \tag{3}$$

$$\frac{dM_{^{20}\mathrm{Ne}}}{dt} = k_3M_{^{16}\mathrm{O}}M_{^4\mathrm{He}} - k_4M_{^{20}\mathrm{Ne}}M_{^4\mathrm{He}} + k_{11}M_{^{24}\mathrm{Mg}} - k_{12}M_{^{20}\mathrm{Ne}}, \tag{4}$$

$$\frac{dM_{^{24}\mathrm{Mg}}}{dt} = k_4M_{^{20}\mathrm{Ne}}M_{^4\mathrm{He}} - k_5M_{^{24}\mathrm{Mg}}M_{^4\mathrm{He}} + k_6M_{^{12}\mathrm{C}}^2 + k_{10}M_{^{28}\mathrm{Si}} - k_{11}M_{^{24}\mathrm{Mg}}, \tag{5}$$

$$\frac{dM_{^{28}\mathrm{Si}}}{dt} = k_5M_{^{24}\mathrm{Mg}}M_{^4\mathrm{He}} + k_7M_{^{12}\mathrm{C}}M_{^{16}\mathrm{O}} - k_9M_{^{28}\mathrm{Si}}M_{^4\mathrm{He}}^7 - k_{10}M_{^{28}\mathrm{Si}} + k_{15}M_{^{56}\mathrm{Ni}}, \tag{6}$$

$$\frac{dM_{^{56}\mathrm{Ni}}}{dt} = k_8M_{^{16}\mathrm{O}}^2M_{^4\mathrm{He}}^6 + k_9M_{^{28}\mathrm{Si}}M_{^4\mathrm{He}}^7 - k_{15}M_{^{56}\mathrm{Ni}}. \tag{7}$$

To solve system (1)–(7), we use the `ChemPAK` code [15], which is based on the implicit Euler method of the fifth order of accuracy, known as `RADAU5` in the literature.

2. DISTRIBUTED COMPUTATION SYSTEM

A feature of the study of such a network of nuclear reactions is the possibility of distributed computing for each set of the mass fraction of elements and the temperature and density of the degenerate gas of white dwarfs. To implement distributed computing, we use a client-server architecture. DHCA (Distributed Hydrodynamic Computation Application) is a client-server distributed

computing system consisting of three main components: a server, a web application, and an application based on the Android operating system. The server is responsible for storing and distributing computational units among end Android-based mobile devices. The server stores the results of calculations for each computing block and, upon successful completion of calculations, accumulates the total result of all blocks; it stores basic user information needed to distribute work. The web application is responsible for creating distributed computing tasks, loading initial conditions, tracking the progress of calculations, and uploading the results; it is a closed segment of the system with limited access. The Android application is responsible for processing the computational blocks received from the server according to a certain algorithm; sends the results back to the server; and is responsible for registering users in the system. The work of the application begins with the creation of a task for calculations. With the help of a web application, a specialist enters basic information about a task (name, description, etc.), and also loads the initial conditions of the task in the form of a file of a certain format. When uploading data to the server, the task is divided into a certain number of computational blocks according to the algorithm depending on the type of the task. The number of blocks is determined from the number of active system users or can be set by the specialist when creating the task. The user's work with the Android application begins with registration in the system. When registering, the user enters login and password under which further work will be carried out. When registering, the system establishes connection with the Firebase Cloud Messaging (FCM) platform, which is responsible for working with notifications. A successful connection to this platform is accompanied by the issuance of a unique token for the device using which the server is able to send notifications to a specific device. The token is entered into the user's account and used later on to allocate computing units and maintain statistics. After registration, the user will be able to view and select currently unfinished tasks. After starting a task for calculation, all users of the Android application receive a notification about the appearance of a new task. When a task is selected for calculation, the application sends a request to the server to receive computational blocks. If there are free blocks, the server sends the first available block as a response and reserves it for the user using the FCM token. If there are no free blocks, but there are blocks that are reserved for other users but have not received a result within a day, the server sends the first such block and reserves it for a new user. The application, having received a response from the server, in the case of the presence of computational blocks, writes the response to the local database and starts computing the block in thread-safe code based on Kotlin Coroutines. The user monitors the calculation process and can interrupt it at any time. Also, the user can refuse to participate in the task, in which case all computational blocks reserved for this user that did not receive the result of calculations will be canceled and become available to other users. If the calculation is successful, the result is written to the local database, and then it is sent to the server. In the absence of an Internet connection, the sending of results is interrupted until a connection is established. If the result is successfully sent to the server, the application requests free computational blocks; if there are any, the iteration is repeated until there are free blocks or until the user terminates the application. When the results arrive at the server, the server checks every time if there are still computational blocks for which there is no result; if there are no more such blocks, then the task is considered completed and the server accumulates the final file of a certain format. Further, in this case the task is marked as completed in the web and the Android applications, and the final file becomes available for download in the web interface. Lightweight threads are used to implement the distributed computing system (see Fig. 1).

The system is an implementation of a mixture of a pattern for distributed computing on mobile devices and a map/reduce pattern. Further, this system is reliable, because it redistributes blocks from inaccessible nodes between available devices. On the client side, background calculations are organized using Kotlin Coroutines; with further development, we hope to increase performance with this technology.

At the moment, the client part works on all Android devices starting from version 6.0 (Marshmallow), which gives almost 94% coverage of all Android users. The larger the coverage, the greater the final performance the system will be able to produce. At the same time, the system has a number of nuances. Adding a new type of task requires refining both the web and client parts of the application. In addition, such improvements ultimately require software updates from the end user of the mobile device. Since task types are backward compatible with the application version, a user

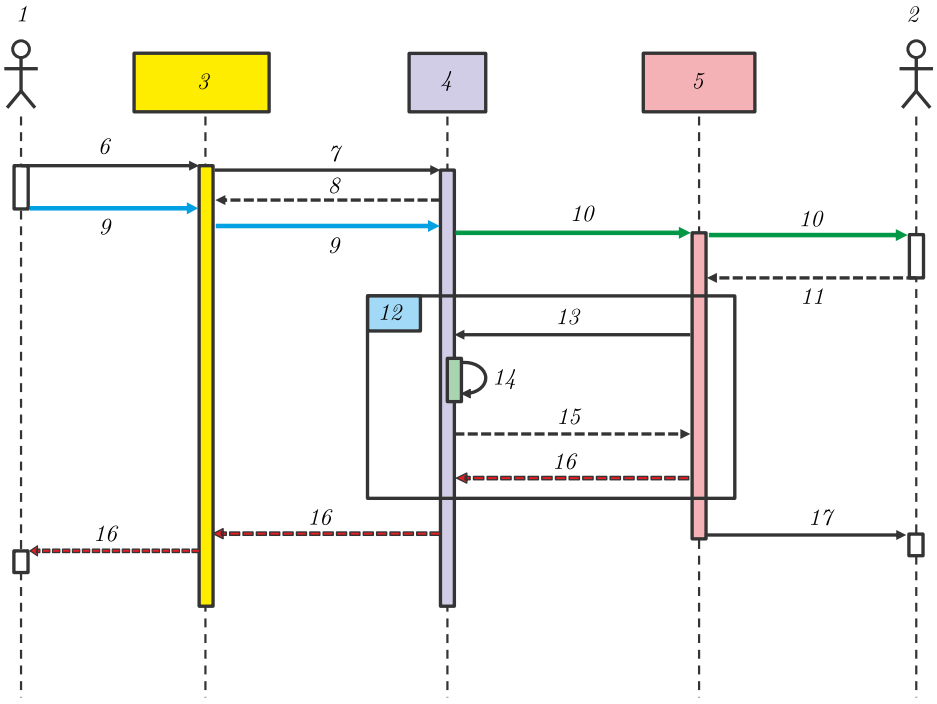

Fig. 1. Conceptual system operation diagram: (*1*) researcher, (*2*) user, (*3*) Web application, (*4*) server, (*5*) mobile application, (*6*) data input, (*7*) data recording, (*8*) data display, (*9*) calculation start, (*10*) a new job notification, (*11*) acceptance, (*12*) loop, (*13*) data request, (*14*) check for availability of free data, (*15*) data transmission, (*16*) result, (*17*) displaying the result.

with an older version of the client will not be able to participate in the new type of task. The specialist who opens the task must know the format of the parameter file for each type of the task. This shortcoming can be solved by further improvement of the web application in terms of entering task parameters, highlighting required fields, and automatically generating a parameter file based on the data entered. It is also worth noting that with the proper level of abstraction and parameterization of each type of problem at the design stage, it is possible to achieve great variability in terms of setting the conditions.

3. COMPUTATIONAL EXPERIMENTS

As the most significant, let us consider four computational experiments: combustion of low-density carbon, combustion of high-density carbon, combustion of high-density carbon and oxygen, and intensive combustion of high-density carbon. We note that we will consider most of the results on the evolution of the mass fraction not only on a linear but also on a logarithmic scale. This is due to the fact that the characteristic hydrodynamic time in the explosion of type Ia supernovae is approximately 10^3 s, and the characteristic time of explosion of type Ia supernovae is approximately 1–10 s. Nevertheless, the process does not end with a supernova explosion, and we will consider the evolution of the change in the mass fraction up to times of the order of several dozens of years, during which the remnant is formed.

For the first computational experiment, we consider a degenerate gas consisting entirely of carbon ^{12}C with density $\rho = 10^7$ g/cm^3 and temperature $T = 10^9$ K. This condition is the lower limit of carbon combustion in terms of density and temperature. The results of modeling the evolution of the mass fraction of M elements over time t in seconds are shown in Fig. 2.

Modeling shows that during the characteristic time of formation of supernova explosion remnants with the minimum allowable carbon combustion parameters, the main combustion products are 28%

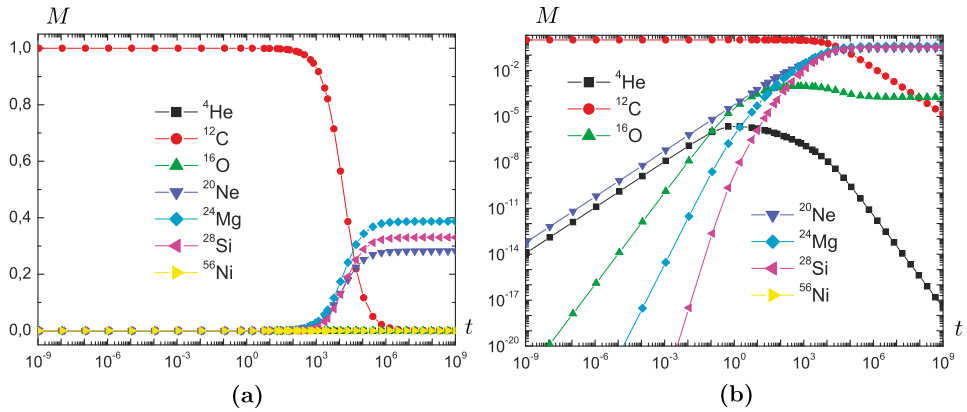

Fig. 2. Change in the mass fraction of elements during carbon combustion at the minimum allowable values of density and temperature for the first experiment on linear (a) and logarithmic (b) scales.

neon, 38% magnesium, and 33% silicon, while the remaining elements do not exceed one percent. The formation of neon occurs owing to the combustion of carbon and the photodisintegration of magnesium at the initial times, then the main source of neon is the combustion of oxygen with the consumption of the helium isotope. As soon as the helium runs out, the production of neon also stops. Combustion of carbon and bonds of carbon and oxygen make it possible to obtain a high content of magnesium and silicon. Note that at hydrodynamic times, the formation of elements is fairly well described by a linear function for logarithmic values of the mass fraction and time. Thus, the mass fraction is approximately described by the function $M = 10^A \times t^B$. Note also that under these conditions there is no formation of nickel. Using the least squares method, we determined the following approximate functions for the change in mass fraction over the hydrodynamic time:

$$M_{^4\mathrm{He}} = 1.122 \times 10^{-5} \times t^{0.9997}, \quad M_{^{16}\mathrm{O}} = 0.776 \times 10^{-6} \times t^{1.6392}, \quad M_{^{20}\mathrm{Ne}} = 6.623 \times 10^{-5} \times t^{1.0007},$$
$$M_{^{24}\mathrm{Mg}} = 0.158 \times 10^{-14} \times t^{1.1106}, \quad M_{^{28}\mathrm{Si}} = 0.316 \times 10^{-23} \times t^{1.4256}.$$

Note that the formation of magnesium and silicon over hydrodynamic times is rather small, while at times of the order of formation of the remnant, these elements determine the main mass fraction of elements.

In the second computational experiment, we also consider a gas consisting entirely of carbon ^{12}C with a density $\rho = 10^9$ g/cm^3 typical for the detonation region and a combustion temperature carbon $T = 10^9$ K. The results of modeling the evolution of the mass fraction M of elements over time t in seconds for the second experiment are shown in Fig. 3.

Modelling shows that the behavior of the mass fraction of isotopes corresponds qualitatively to the previous experiment. The main difference lies in the formation of the mass fraction of the remnants of a supernova explosion, the values of which reach 29% for neon, 34% for magnesium, and 36% for silicon, while the rest of the elements also do not exceed one percent. Approximate functions for the change the mass fraction over the hydrodynamic time take the following form:

$$M_{^4\mathrm{He}} = 1.701 \times 10^{-2} \times t^{0.9857}, \quad M_{^{16}\mathrm{O}} = 3.539 \times 10^{-2} \times t^{1.9514}, \quad M_{^{20}\mathrm{Ne}} = 1.254 \times 10^{-1} \times t^{0.9998},$$
$$M_{^{24}\mathrm{Mg}} = 0.576 \times 10^{-3} \times t^{1.1107}, \quad M_{^{28}\mathrm{Si}} = 0.281 \times 10^{-9} \times t^{1.5264}.$$

Note that, compared with the previous experiment, the main difference in the laws of change in the mass fraction is in the powers of the coefficient multiplying the exponential function of time.

For the third experiment, we retain the density and temperature parameters from the second experiment, but consider a gas with equal mass fractions of oxygen and carbon. The results of modeling the evolution of the mass fraction M of elements over time t in seconds for the third experiment are shown in Fig. 4.

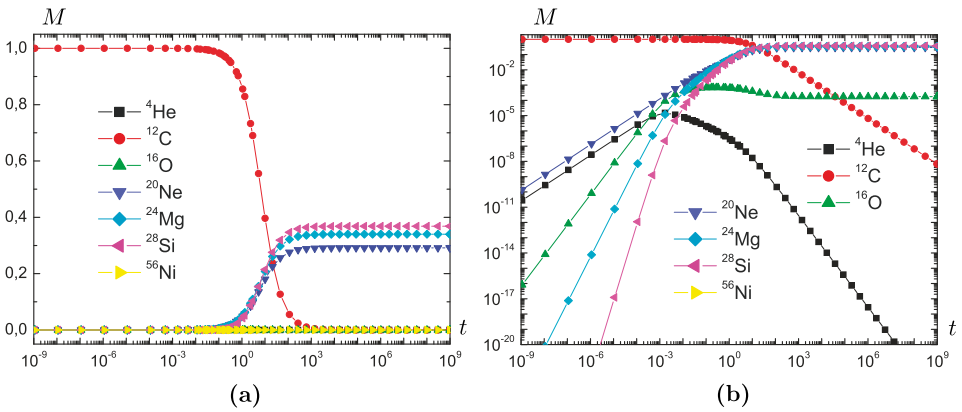

Fig. 3. Change in the mass fraction of elements during carbon combustion at the minimum allowable values of density and temperature for the second experiment on linear (a) and logarithmic (b) scales.

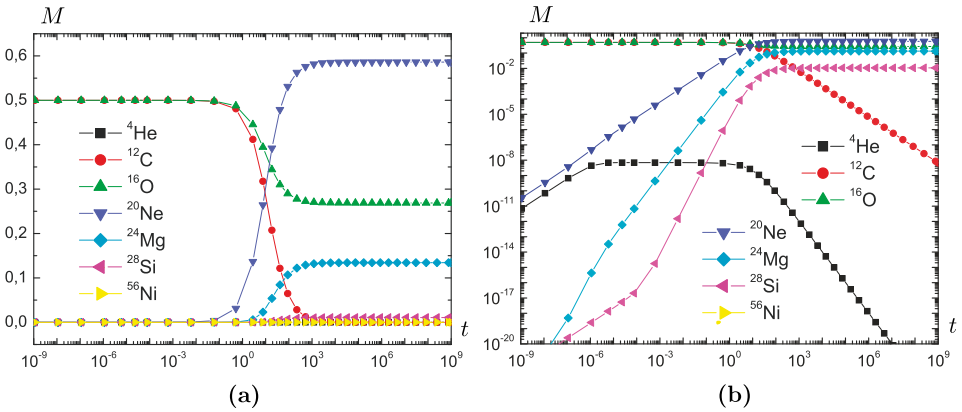

Fig. 4. Change in the mass fraction of elements during carbon combustion with the minimum allowable values of density and temperature for the third experiment on linear (a) and logarithmic (b) scales.

The results of the experiment showed that during the formation of the residue, the mass fraction of oxygen drops from 50% to 27%, while the mass fraction of neon reaches 58%, which occurs mainly due to the combustion of oxygen. The mass fraction of magnesium falls in comparison with the previous experiments to 13% and that of silicon to 2%, mainly due to the lower mass fraction of carbon. Note that the change in the mass fraction of silicon, magnesium, and neon corresponds to the previous experiment over short times. We note that for equal masses of carbon and oxygen, the mass fraction of the helium isotope reaches its maximum in a particularly pronounced way.

In the fourth experiment, we consider the limit case of carbon combustion at a temperature of $T = 10^{10}$ K with density $\rho = 10^9$ g/cm^3, typical for the detonation region. The results of modeling the evolution of the mass fraction of M elements over time t in seconds for the fourth experiment are shown in Fig. 5.

Within the characteristic hydrodynamic time, all carbon combustion reactions occur with intermediate formation of isotopes including nickel. Thus, we have a substantial temperature interval from 10^9 to 10^{10} K on which the exponent for the change of the mass fraction of elements depends. In the next section, as a discussion, we will propose one approximation to the change in the mass fraction of elements that can be used to construct a subgrid combustion process of a material.

4. DISCUSSION

As part of the discussion, we present a subgrid model of the combustion of white dwarf material. Of course, we are constructing only an approximate model of nuclear reactions, which is able to

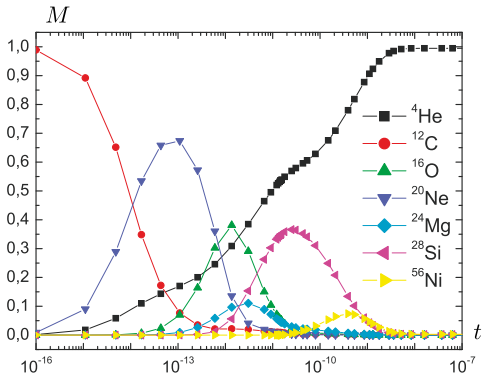

Fig. 5. Change in the mass fraction of elements during the combustion of carbon with a characteristic density and high temperature in the fourth experiment.

describe quite well the change in the mass fraction of elements in the first approximation. This will allow us to considerably reduce computational costs for the description of nuclear reactions, since their computation in one cell over the characteristic hydrodynamic time requires approximately a second. Since for tens of thousands of time steps in each of approximately a billion computational cells we will use an analytic function instead of calculating the ODE system (1)–(7), such a problem can be fundamentally calculated on available supercomputers in the three-dimensional setting. In the future, we plan to present the results of similar calculations using such a model. Here are the main assumptions when constructing the "convolution":

1. At a temperature of the order of $T = 10^{10}$ K over times of the order of 10^{-10} c, we will use Gaussian functions to change the mass fraction of the elements of the alpha chain of nuclear reactions.
2. We will use a sigmoid to go from the temperature $T = 10^9$ K to the temperature $T = 10^{10}$ K.
3. Let us take into account the experimental fact that 50% of the formation of neon occurs due to the combustion of oxygen.
4. Carbon and oxygen are the main sources of formation of all elements, while oxygen is "responsible" only for the formation of neon.
5. To be definite, we consider the change in the coefficients in the mass fraction of isotopes to be linear in the decimal logarithm of the density.
6. It is stated in the paper [1] that the 7-isotope model of nuclear reactions is sufficient from the point of view of describing the energy of combustion.
7. Undoubtedly, such a small set of isotopes does not fully describe the chemical diversity of the composition. In particular, when considering nickel, we are not talking about nickel itself but about the isotopes of the iron group. In fact, we fully describe the material of white dwarfs (carbon, oxygen, neon), the first elements of combustion (magnesium and silicon), and also the iron group (nickel). However, we believe that such a composition is sufficient to describe the combustion energy as well as to describe the chemical composition of the main elements of the interstellar medium.

Let us define dimensionless variables $T9 = T/10^9$ K, temperature in 10^9 K, ρ — density in g/cm^3, and t, time in seconds, as well as two auxiliary functions:

$$\sigma(T) = \frac{1}{1 + e^{-2\times T9+10}}, \quad g(t,\mu,c) = \frac{1}{c\sqrt{2\pi}} e^{-(t-\mu)/(2c^2)},$$

which we will use to describe changes in the mass fractions of isotopes. Here are the formulas for how they change:

$$\frac{dM_{^4\mathrm{He}}}{dt} = \sigma(T) \times g\left(t, 10^{-3}, 1/\sqrt{2\pi}\right) + \big(1 - \sigma(T)\big)\big((0.0085 \times \lg\rho - 0.0594) \times t^{1.0487 - 0.007\times\lg\rho}\big),$$

$$\frac{dM_{^{12}\mathrm{C}}}{dt} = -\frac{dM_{^{4}\mathrm{He}}}{dt} - \frac{dM_{^{16}\mathrm{O}}}{dt} - \frac{dM_{^{20}\mathrm{Ne}}}{dt} - \frac{dM_{^{24}\mathrm{Mg}}}{dt} - \frac{dM_{^{28}\mathrm{Si}}}{dt} - \frac{dM_{^{56}\mathrm{Ni}}}{dt},$$

$$\frac{dM_{^{16}\mathrm{O}}}{dt} = \sigma(T) \times g\left(t, 10^{-12}, 3/\sqrt{2\pi}\right) + \big(1-\sigma(T)\big)\big((0.0176 \times \lg\rho - 0.1238) \times t^{0.5465+0.1561\times\lg\rho}\big) - \frac{M_{^{16}\mathrm{O}}}{5+5e^{\lg t+3}},$$

$$\frac{dM_{^{20}\mathrm{Ne}}}{dt} = \sigma(T) \times g\Big(t, 10^{-13}, 1/\sqrt{\pi}\Big) + \big(1-\sigma(T)\big)\big((0.0627 \times \lg\rho - 0.4386) \times t^{1.0038-0.0004\times\lg\rho}\big) + \frac{M_{^{16}\mathrm{O}}}{5+5e^{\lg t+3}},$$

$$\frac{dM_{^{24}\mathrm{Mg}}}{dt} = \sigma(T) \times g(t, 10^{-11}, 3) + \big(1-\sigma(T)\big)\big((0.00029 \times \lg\rho - 0.0021) \times t^{1.1102-0.00005\times\lg\rho}\big),$$

$$\frac{dM_{^{28}\mathrm{Si}}}{dt} = \sigma(T) \times g\left(t, 10^{-10}, 3/\sqrt{2\pi}\right) + \big(1-\sigma(T)\big)\big(10^{-9}(0.1405 \times \lg\rho - 0.9835) \times t^{1.0728+0.0504\times\lg\rho}\big),$$

$$\frac{dM_{^{56}\mathrm{Ni}}}{dt} = \sigma(T) \times g(t, 10^{-9}, 4).$$

These approximate functions can be used to change the mass fraction of isotopes at times from $t = 10^{-15}$ s to $t \approx 1$ s, which permits one to describe explosion processes not only at the initial stages of combustion but also over the characteristic times of a type Ia supernova explosion and over times of the order of formation of the remnant.

Consider an equilibrium solution of the original ODE system (1)–(7) by equating the left-hand side of the equations with zero. In addition, we set the condition $M_{^{4}\mathrm{He}} = 0$; i.e., alpha particles are considered exhausted. This leads to the equality $M_{^{56}\mathrm{Ni}} = 0$, which indicates the absence of isotopes of the iron group when alpha particles are exhausted. We will go even further and exclude neon and magnesium from consideration; i.e., we set $M_{^{20}\mathrm{Ne}} = 0$ and $M_{^{24}\mathrm{Mg}} = 0$. This permits us to write the following relations:

$$k_7 M_{^{12}\mathrm{C}} M_{^{16}\mathrm{O}} = k_{10} M_{^{28}\mathrm{Si}},$$
$$k_{13} M_{^{16}\mathrm{O}} = 2k_6 M_{^{12}\mathrm{C}}^2 + k_7 M_{^{12}\mathrm{C}} M_{^{16}\mathrm{O}} + k_{14} M_{^{12}\mathrm{C}}.$$

As a result, we arrive at one equilibrium state

$$k_{13} M_{^{16}\mathrm{O}} = 2k_6 M_{^{12}\mathrm{C}}^2 + k_{10} M_{^{28}\mathrm{Si}} + k_{14} M_{^{12}\mathrm{C}}.$$

Such a state determines the incomplete combustion of a carbon-oxygen dwarf with the formation of a silicon isotope that underlies interstellar dust.

CONCLUSIONS

A "convolution" of alpha network of nuclear reactions for a 7-isotope system is proposed. The isotopes of helium, carbon, oxygen, neon, magnesium, silicon, and nickel are considered. The model of nuclear reactions based on many computational experiments was written in a fairly simple analytical form that can be used in a hydrodynamic model of the evolution of white dwarfs and the explosion of type Ia supernovae.

FUNDING

This work was supported by the Russian Science Foundation, project no. 18-11-00044, https://rscf.ru/project/18-11-00044/.

REFERENCES

1. F. X. Timmes, R. D. Hoffman, and S. E. Woosley, "An inexpensive nuclear energy generation network for stellar hydrodynamics," Astrophys. J. Suppl. Ser. **129**, 377–398 (2000).

2. P. Zhou, S.-C. Leung, Z. Li, K. Nomoto, J. Vink, and Y. Chen, "Chemical abundances in Sgr A East: evidence for a type Iax supernova remnant," Astrophys. J. **908**, 31 (2021).
3. S.-C. Leung and K. Nomoto, "Explosive nucleosynthesis in near-Chandrasekhar mass white dwarf models for type Iax supernovae: Dependence on model parameters," Astrophys. J. **900**, 54 (2020).
4. I. M. Kulikov, I. G. Chernykh, and A. V. Tutukov, "Mathematical modeling of a high-speed collision of white dwarfs—the explosion mechanism of type Ia/Iax supernovae," Sib. Zh. Ind. Mat. **25** (1), 80–88 (2022) [J. Appl. Ind. Math. **16** (1), 80–88 (2022)].
5. C. Kobayashi, S.-C. Leung, and K. Nomoto, "New type Ia supernova yields and the manganese and nickel problems in the Milky Way and dwarf spheroidal galaxies," Astrophys. J. **895**, 138 (2020).
6. A. Tanikawa, K. Nomoto, and N. Nakasato, "Three-dimensional simulation of double detonations in the double-degenerate model for type Ia supernovae and interaction of ejecta with a surviving white dwarf companion," Astrophys. J. **868**, 90 (2018).
7. A. Tanikawa, K. Nomoto, N. Nakasato, and K. Maeda, "Double-detonation models for type Ia supernovae: Trigger of detonation in companion white dwarfs and signatures of companions' stripped-off materials," Astrophys. J. **885**, 103 (2019).
8. S.-C. Leung and K. Nomoto, "Explosive nucleosynthesis in near-Chandrasekhar-mass white dwarf models for type Ia supernovae: Dependence on model parameters," Astrophys. J. **861**, 143 (2018).
9. S. E. Woosley, A. R. Kerstein, and A. J. Aspden, "Flames in type Ia supernova: Deflagration-detonation transition in the oxygen-burning flame," Astrophys. J. **734**, 37 (2011).
10. S. I. Glazyrin, S. I. Blinnikov, and A. Dolgov, "Flame fronts in type Ia supernovae and their pulsational stability," Mon. Not. R. Astron. Soc. **433**, 2840–2849 (2013).
11. L. Iapichino, M. Brueggen, W. Hillebrandt, and J. C. Niemeyer, "The ignition of thermonuclear flames in type Ia supernovae," Astron. & Astrophys. **450**, 655–666 (2006).
12. N. Arash, G. Peyman, and L. Danie, "Modeling and simulation of turbulent nuclear flames in type Ia supernovae," Progr. Aerosp. Sci. **108**, 156–179 (2019).
13. I. M. Kulikov, "Mathematical simulation of turbulent combustion of carbon in the problems of white dwarf mergers and explosions of type Ia supernovae," Sib. Zh. Ind. Mat. **24** (3), 30–38 (2021). [J. Appl. Ind. Math. **15** (3), 437–442 (2021)].
14. W. A. Fowler, G. R. Caughlan, and B. A. Zimmerman, "Thermonuclear reaction rates, II," Annu. Rev. Astron. Astrophys. **13**, 69–112 (1975).
15. I. Chernykh, O. Stoyanovskaya, and O. Zasypkina, "ChemPAK software package as an environment for kinetics scheme evaluation," Chem. Prod. Process Model. **4** (4), 3 (2009).